Parametric amplification and squeezing with ac- and dc-voltage biased superconducting junction

Udson C. Mendes,[1,2,*] Philippe Joyez,[2] Bertrand Reulet,[1] Alexandre Blais,[1,3]
Fabien Portier,[2] Christophe Mora,[4] and Carles Altimiras[2]

[1]*Institut quantique and Département de Physique, Université de Sherbrooke, Sherbrooke, Québec J1K 2R1, Canada*
[2]*Service de Physique de l'Etat Condensé, CEA, CNRS,*
Université Paris-Saclay, CEA Saclay, 91191 Gif-sur-Yvette, France
[3]*Canadian Institute for Advanced Research, Toronto, Canada*
[4]*Laboratoire Pierre Aigrain, École normale supérieure, PSL Research University, CNRS,*
Université Pierre et Marie Curie, Sorbonne Universités, Université Paris Diderot,
Sorbonne Paris-Cité, 24 rue Lhomond, 75231 Paris Cedex 05, France

(Dated: February 22, 2018)

We theoretically investigate a near-quantum-limited parametric amplifier based on the non-linear dynamics of quasiparticles flowing through a superconducting-insulator-superconducting junction. Photon-assisted tunneling, resulting from the combination of dc- and ac-voltage bias, gives rise to a strong parametric interaction for the electromagnetic modes reflected by the junction coupled to a transmission line. We show phase-sensitive and phase-preserving amplification, together with single- and two-mode squeezing. For an Aluminum junction pumped at 8 GHz, we predict narrow-band phase-sensitive amplification of microwaves signals to more than 30 dB, and broadband phase-preserving amplification larger than 15 dB over a 4 GHz band. We also predict single-mode squeezing reaching -20 dB and two-mode squeezing of -14 dB over a 4 GHz band. A key feature is that the device parameters can be tuned in-situ by the applied dc- and ac-voltage biases.

I. INTRODUCTION

Many of the advances of quantum computation based on superconducting qubits rely on the ability to readout the qubit state by measuring microwave photons leaking out of a superconducting resonator [1]. Thanks to the development of near-quantum-limited Josephson parametric amplifiers (JPAs) [2–5], high-fidelity single-shot qubit readout is now possible [6, 7]. These amplifiers are, moreover, finding use in a wide range of applications, from measuring quantum features in the radiation emitted by mesoscopic conductors [8–12], to the detection of small ensembles of electronic spins [13], and even to the search for dark matter [14]. JPAs are also versatile sources of single- and two-mode squeezed states [5, 15], which have been used to confirm decade old predictions in quantum optics [16, 17], and to improve electron-spin resonance spectroscopy [13]. On the theoretical side, squeezed states were proposed as a resource to improve qubit readout and to perform high-fidelity gates [18–20], or as a basis for continuous variable quantum computing [21, 22].

Current JPAs are able to amplify signals to more than 20 dB, and to squeeze vacuum fluctuations by 7 dB (12 dB) in single- (two-) mode experiments [5, 23]. However, in this devices, the amplification bandwidth is limited to hundreds of megahertz [24–26]. At the price of increasing device fabrication complexity, much larger amplification bandwidth, over ~ 3 GHz, has been demonstrated with the recently developed Josephson traveling wave parametric amplifier [27]. The development of a simpler quantum-limited microwave amplifier, generating far-separated two-mode squeezed states and capable of amplifying signals over gigahertz bandwidths, is still needed to further advance quantum information processing science. It would also be an important tool to better characterize the radiation emitted by mesoscopic conductors, for which there is an increasing body of interesting predictions [28–32]. Here, we propose such a simple broadband parametric amplifier, consisting of a single dc- and ac-voltage biased superconductor-insulator-superconductor (SIS) junction. The device can be operated in both phase-sensitive and phase-preserving modes and can be used for near-quantum-limited amplification and two-mode squeezing in few GHz bandwidth.

The proposed setup, illustrated in Fig. 1(a), operates as an amplifier in reflection mode. Parametric amplification is possible by taking advantage of the strong non-linearity of the transport characteristics of the junction. To this end, we consider a dc-voltage bias V smaller than twice the superconducting gap Δ. This sets the junction as an open circuit, and the conduction of quasiparticles is enabled by applying a sinusoidal ac-voltage $V_{\rm ac}(t) = V_{\rm ac}\cos(2\omega_0 t)$, with ω_0 the measurement center frequency. This voltage combination gives rise to modulations of the admittance of the junction $Y_n(\omega)$, with n the n-th harmonic of the pump. As illustrated in Fig. 1(b), the finite-frequency admittance for dc-voltage approaching $(2\Delta - \hbar\omega_0)/e$ is dominated by a large non-linear susceptance ${\rm Im}Y_1(\omega_0)$ [33, 34]. On the other hand, the dissipative term, ${\rm Re}Y_0(\omega_0)$, is only weakly affected by the ac-voltage and it is dominant for $eV > 2\Delta - \hbar\omega_0$. Taking advantage of dc-voltage control, we demonstrate that parametric amplification and squeezing emerges when $Y_1(\omega_0)$ is much larger than ${\rm Re}Y_0(\omega_0)$. As we show below, $Y_1(\omega_0)$ is related to the coherent conversion process of $2\hbar\omega_0$ quanta of energy from the pump to two photons of frequency ω_0, while ${\rm Re}Y_0(\omega_0)$ is related to dissipative effects due to the tunneling of quasiparticles. It is surprising that even though SIS junctions are routinely used as high-frequency microwave quantum-limited mixers [35], exploiting a very similar principle, their operation as parametric amplifiers have been mostly

* udson.cabral.mendes@usherbrooke.ca

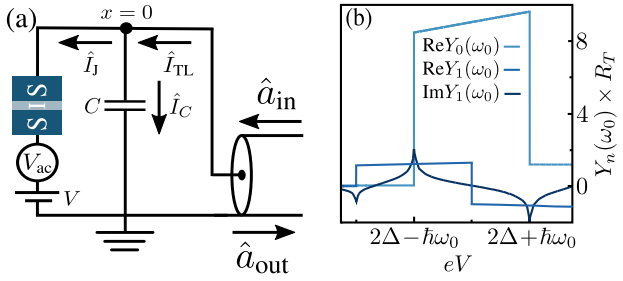

FIG. 1. (a) Electrical scheme of the device: a SIS junction is dc-voltage biased close to the onset of quasiparticle transport $eV \sim 2\Delta$, while it is ac pumped with a single tone $V_{ac}\cos(2\omega_0 t)$. Current conservation at the coupling mode ($x = 0$) allows to relate the transmission line outgoing field $a_{out}[\omega]$ with its incoming field $a_{in}[\omega]$ and the current flowing through the junction $\hat{I}_J[\omega]$. (b) Non-linear admittance as a function of the dc-voltage for an Aluminum junction ($\Delta = 180\ \mu$eV) and $eV_{ac} = 0.135 \times 2\hbar\omega_0$. On one hand, as shown in Sec. II, dissipation emerges from the absorption and emission of photons, which is illustrated by $\mathrm{Re}Y_0(\omega)$. Notably, $\mathrm{Re}Y_0(\omega)$ is only slightly perturbed by such small ac pumping. However, the pumping gives rise to a parametric interaction characterized by a sizable non-linear admittance $Y_1(\omega_0)$. For dc-voltages in the range $2(\Delta - \hbar\omega_0) < eV < 2\Delta - \hbar\omega_0$, the non-linear admittance $Y_1(\omega_0)$ dominates over the dissipative response $\mathrm{Re}Y_0(\omega)$ giving rise to parametric amplification and squeezing.

disregarded [34, 36]. Here, we use the input-output formalism [37], together with photon-assisted tunneling theory [38] to compute the parametric amplification and squeezing properties of an ac- and dc-biased SIS junction [35]. The resulting Heisenberg-Langevin equations [39] are numerically solved, allowing us to explore parametric amplification far from the small detuning limit considered previously [34, 36]. For an Aluminum junction ($\Delta = 180\ \mu$eV) pumped at $2\omega_0 = 8$ GHz and operated at temperatures $T \ll \Delta/k_B$, with k_B the Boltzmann constant, we find that when operated in the phase-sensitive mode this device can produce more than 30 dB of gain and -20 dB of squeezing. On the other hand, operated in the phase preserving-mode, it achieves 15 dB of gain with an added noise close to the quantum limit and -14 dB of two-mode squeezing, in both cases over a large bandwidth exceeding 4 GHz. Moreover, the gain and the squeezing bandwidths are easily tuned by the dc-voltage and ac-pumping, allowing for instance to achieve higher gain in a reduced yet sizable bandwidth.

This article is organized as follows: In Sec. II we describe the input-output formalism used to characterize the device. Section III A presents the results for an ideal SIS junction for which the transport response rises steeply for $eV = 2\Delta + n\hbar\omega_0$. The effects of the low-frequency noise, which captures most non-ideal effects, on the amplifier is described in Sec. III B. Final remarks are presented in Sec. IV.

II. MODEL

We consider a SIS junction in parallel with its capacitance C and connected to a transmission line (TL), see Fig. 1(a). The Hamiltonian of the device is $\hat{H} = \hat{H}_{qp} + \hat{H}_{ee} + \hat{H}_t$, where $\hat{H}_{qp}$ describes the quasiparticles in the superconductors forming the junction, $\hat{H}_{ee}$ is the electromagnetic environment Hamiltonian, which includes the TL and the capacitor C of the junction. The last term is the tunneling Hamiltonian dressed by the environment and takes the form $\hat{H}_t = \hat{\mathcal{T}}(t)\exp[ie\hat{\Phi}(t)/\hbar] + \text{h.c.}$ with [40]

$$\hat{\mathcal{T}}(t) = \sum_{l,r} t_{lr}\hat{c}_l^\dagger \hat{c}_r e^{i[eVt/\hbar + \varphi_{ac}(t)]}, \tag{1}$$

the tunneling operator transferring a quasiparticle from the right (r) to the left (l) side of the junction. In this expression, $\hat{c}_{r(l)}$ is the annihilation operator of a quasiparticle in the right (left) superconductor and $t_{lr} \equiv t_{rl}$ the tunneling probability amplitude. The phase $\varphi_{ac}(t) = (eV_{ac}/2\hbar\omega_0)\sin(2\omega_0 t)$ takes into account the ac-voltage. Finally, $\hat{\Phi}(t) \equiv \hat{\Phi}(t, x = 0)$ is the TL flux at the position of the junction. In the interaction picture with respect to $\hat{H}_t$, this flux is written in terms of the incoming $\hat{a}_{in}[\omega]$ and outgoing $\hat{a}_{out}[\omega]$ fields as [37]

$$\hat{\Phi}(t,x) = \sqrt{\frac{\hbar Z_0}{4\pi}}\int_0^\infty \frac{d\omega}{\sqrt{\omega}}\Big[\hat{a}_{in}[\omega]e^{-i(\omega t + k_\omega x)} + \hat{a}_{out}[\omega]e^{-i(\omega t - k_\omega x)} + \text{ h.c.}\Big], \tag{2}$$

with $k_\omega = \omega\sqrt{L_0 C_0}$ the wave number and $Z_0 = \sqrt{L_0/C_0}$ the TL impedance defined in terms of its inductance L_0 and capacitance C_0 per unity of length. The incoming (outgoing) field obeys the commutation relation $[\hat{a}_{in\ (out)}[\omega], \hat{a}^\dagger_{in\ (out)}[\omega']] = \delta(\omega - \omega')$.

To characterize the radiation emitted by the junction, we use the input-output formalism adapted to circuits coupled to quantum conductors [30, 41, 42]. To obtain the input-output boundary condition, the first step is to derive the Heisenberg equations of motions for both TL charge and flux at the position of the junction ($x = 0$). The resulting equations are combined to express current conservation

$$C\ddot{\hat{\Phi}}(t, x = 0) - \frac{1}{L_0}\frac{\partial\hat{\Phi}(t,x)}{\partial x}\bigg|_{x=0} = \hat{I}_J(t), \tag{3}$$

which connects the outgoing field to the incoming field and the current of the junction $\hat{I}_J(t)$. Using Eq. (2), the above equation can be expressed as an input-output relation

$$\hat{a}_{out}[\omega] = \frac{1 + iZ_0 C\omega}{1 - iZ_0 C\omega}\hat{a}_{in}[\omega] + i\sqrt{\frac{Z_0}{\pi\hbar\omega}}\frac{\hat{I}_J[\omega]}{1 - iZ_0 C\omega}, \tag{4}$$

where $\hat{I}_J[\omega]$ is the Fourier transform of $\hat{I}_J(t)$. The current $\hat{I}_J[\omega]$ depends not only on the dc- and ac-voltages, but also on the TL voltage, $\hat{V}_{TL}(t) = \dot{\hat{\Phi}}(t)$, implying that $\hat{I}_J[\omega]$ and $\hat{a}_{in}[\omega]$ do not commute. To circumvent the non-commutation

between $\hat{I}_{\rm J}[\omega]$ and $\hat{a}_{\rm in}[\omega]$, we take advantage of the weak TL-junction coupling $\sqrt{\pi Z_0/R_K} \ll 1$ (for a typical $Z_0 = 50\Omega$ TL impedance, with $R_K \simeq 25.8$ kΩ the quantum of resistance), and compute $\hat{I}_{\rm J}[\omega]$ to second-order in the TL-junction coupling [31, 41]. In the time-domain and for weak coupling to the environment, the current operator takes the form

$$\hat{I}_{\rm J}(t) = \hat{I}_{\rm qp}(t) + \frac{e^2}{\hbar^2}\hat{H}^{\rm t}_{\rm qp}(t)\hat{\Phi}(t), \tag{5}$$

where $\hat{I}_{\rm qp}(t) = i(e/\hbar)(\hat{\mathcal{T}}^\dagger(t) - \text{h.c.})$ and $\hat{H}^{\rm t}_{\rm qp}(t) = \hat{\mathcal{T}}(t) + \text{h.c.}$ are respectively the quasiparticle current and tunneling operators in the absence of TL voltage. The final step is to time-evolve $\hat{I}_{\rm J}(t)$. Using linear response theory, the quasiparticles operators are time-evolved, in the interaction picture, with the interaction Hamiltonian $H_{\rm int}(t) = -\hat{I}_{\rm qp}(t)\hat{\Phi}(t)$. Once more, we take advantage of the weak TL-junction coupling to expand the time-evolution operator to first-order. We further neglect quantum fluctuations of the current operator, and average over the quasiparticle operators in the terms proportional to $\hat{\Phi}(t)$. Under these approximations, the current operator is written in frequency space as

$$\hat{I}_{\rm J}[\omega] = \hat{I}_{\rm qp}[\omega] + \sum_n Y_n(\omega - 2n\omega_0)\hat{V}_{\rm TL}[\omega - 2n\omega_0], \tag{6}$$

with $\hat{I}_{\rm qp}[\omega]$ and $\hat{V}_{\rm TL}[\omega]$ the Fourier transforms of $\hat{I}_{\rm qp}(t)$ and $\hat{V}_{\rm TL}(t)$, respectively. The generalized admittance

$$Y_n(\omega) = -\frac{i}{\hbar}\int \frac{d\omega_1}{2\pi}\frac{S_n(\omega) - S_n(2n\omega_0 - \omega)}{(\omega_1 + \omega + i0^+)(\omega_1 + i0^+)}, \tag{7}$$

relates the current response at frequency ω to the TL-voltage dynamics at frequency $\omega - 2n\omega_0$ [42]. The admittance is defined in terms of the photon-assisted current-current correlator $\langle \hat{I}_{\rm qp}(\omega)\hat{I}_{\rm qp}(\omega')\rangle = 2\pi\sum_n S_n(\omega)\delta(\omega + \omega' - 2n\omega_0)$ where

$$S_n(\omega) = \frac{1}{2}\sum_{n_1=-\infty}^{\infty} J_{n_1}(\rho)[J_{n_1+n}(\rho)S_{\rm eq}(\hbar\omega + eV + 2n_1\hbar\omega_0) + J_{n_1-n}(\rho)S_{\rm eq}(\hbar\omega - eV - 2n_1\hbar\omega_0)] \tag{8}$$

is non-symmetrized photon-assisted current noise [31, 41, 42]. It is defined in terms of the Bessel function $J_n(\rho = eV_{\rm ac}/2\hbar\omega_0)$ and of the equilibrium current noise $S_{\rm eq}(\omega) = 2e\langle\hat{I}_{{\rm qp},\omega}\rangle/[1 - \exp(-\hbar\omega/k_{\rm B}T)]$, with $\langle\hat{I}_{{\rm qp},\omega}\rangle$ is the SIS junction quasiparticle current [43].

Equation (6) describes the linear response of the junction due to TL-voltage fluctuations. In the absence of ac-voltage, the linear response is strictly local in frequency with $Y_{n\neq 0}(\omega) = 0$. On the other hand, the addition of the ac-bias enables the response of $Y_{n\neq 0}(\omega) \neq 0$ due to TL-voltage fluctuations at frequencies beating with the harmonics of the pump frequency $2n\omega_0$. It is important to mention that $Y_{n\neq 0}(\omega)$ is only different of zero for non-linear junctions [42]. Consequently, in this device, parametric interaction is due to the combination of both photon-assisted transport and non-linearity. For instance, the non-linearity converts a single pump photon of frequency $2\omega_0$ into two photons of frequency ω_0 [44]. In the SIS amplifier, this process is given by $\text{Im}Y_1(\omega)$, which describes the coherent conversion of $2\hbar\omega_0$ quantum of energy from the pump to two photons of frequency ω_0 [31]. As the junction absorbs photons, thereby introducing losses, the SIS amplifier has to be operated in the dc-voltage range in which parametric interaction, which is related to $Y_1(\omega_0)$, dominates over dissipative effects $\propto \text{Re}Y_0(\omega_0)$. Fig. 1(b) illustrates the dc-voltage dependence of $Y_1(\omega_0)$ and $\text{Re}Y_0(\omega_0)$ for a weak pump amplitude $eV_{\rm ac} = 0.135 \times 2\hbar\omega_0$. We observe that $Y_1(\omega_0)$ present strong discontinuities at $eV = 2\Delta + n\hbar\omega_0$, which is a characteristic of photon-assisted transport and non-linearity, while $\text{Re}Y_0(\omega_0)$ is weakly affected by the ac-voltage. Moreover, $Y_1(\omega_0)$ is larger than $\text{Re}Y_0(\omega_0)$ for $eV < 2\Delta - \hbar\omega_0$, which sets dc-voltage operational point of the device. Finally, it is important to emphasize that $\hat{I}_{\rm qp}[\omega]$ and $Y_n(\omega - 2n\omega_0)$ depend only on the quasiparticles dynamics determined by $H_{\rm qp} + H^{\rm t}_{\rm qp}(t)$, and on the intrinsic characteristics of the junction, e.g., the superconducting gap Δ and normal state resistance R_T, bias conditions, and temperature.

Finally, replacing Eq. (6) into Eq. (4), we obtain the expression for the outgoing field in terms of the incoming field and of the quasiparticles current operators

$$\hat{a}_{\rm out}[\omega + \omega_0] = r_\omega\hat{a}_{\rm in}[\omega + \omega_0] + \gamma_\omega\hat{a}^\dagger_{\rm in}[\omega_0 - \omega] + \alpha_\omega\hat{I}_{\rm qp}[\omega + \omega_0] + \beta_\omega\hat{I}_{\rm qp}[\omega - \omega_0], \tag{9}$$

where $r_\omega = \Delta_\omega^{-1}[P_{-,\omega+\omega_0}P^*_{+,\omega_0-\omega} + A_\omega]$ is the reflection coefficient, with $P_{\pm,\omega} = \kappa_{\pm,\omega} \mp i\omega$ and $\kappa_{\pm,\omega} = (Z_0^{-1} \pm \text{Re}Y_{0,\omega})/C$ defining the total $(+)$ and effective $(-)$ photon decay rate of the device. Here, terms proportional to Z_0^{-1} and $\text{Re}Y_{0,\omega}$ are the internal TL decay rate at which the junction absorb and emits photons, respectively. The dependence of the reflection coefficient with parametric term is given by $A_\omega = Y_{1,\omega-\omega_0}Y^*_{1,-\omega-\omega_0}/C^2$. Finally, $\Delta_\omega = P_{+,\omega+\omega_0}P^*_{+,\omega_0-\omega} - A_\omega$. Note that, we neglected a frequency shift contribution proportional to $\text{Im}Y_{0,\omega}$. In the second term of Eq. (9), we have introduced $\gamma_\omega = 2(Z_0C\Delta_\omega)^{-1}\sqrt{(\omega_0 - \omega)/(\omega + \omega_0)}Y_{1,\omega-\omega_0}$. Moreover, the coefficients of $\hat{I}_{\rm qp}[\omega \pm \omega_0]$ are $\alpha_\omega = \mu_\omega\Delta_\omega^{-1}P^*_{+,\omega_0-\omega}$, and $\beta_\omega = \mu^*_\omega\Delta_\omega^{-1}Y_{1,\omega-\omega_0}/C$, with $\mu_\omega = i/C\sqrt{\pi Z_0\hbar(\omega + \omega_0)}$.

Equation (9) is a central result of this paper and show that the dc- and ac-voltage biased SIS junction acts as an amplifier operating in reflection mode. More specifically, for a fixed frequency $\omega \neq 0$, the operators $\hat{a}_{\rm in}[\omega + \omega_0]$ and $\hat{a}^\dagger_{\rm in}[\omega_0 - \omega]$ commute and can be seen as the input signal and the idler mode operators of a phase-preserving amplifier [44, 45]. In this mode, the gain is simply given by $G(\omega) = |r_\omega|^2$ and the three last terms of Eq. (9) correspond to added noise, which limits the amplifier quantum efficiency. The added noise is [23, 45]

$$\mathcal{A}(\omega) = \frac{1}{2}\left(1 - \frac{1}{G(\omega)} + \frac{4\pi}{G(\omega)}\left[|\alpha_\omega|^2 S_0(\omega + \omega_0) + |\beta_\omega|^2 S_0(\omega - \omega_0) + 2\text{Re}[\alpha_\omega\beta^*_\omega]S_1(\omega + \omega_0)\right]\right), \tag{10}$$

where the first two terms describe the noise added of an ideal phase-preserving amplifier. The remaining terms are noise

generated by the tunneling of quasiparticles, and they originate from absorption and emission processes of one and two quantum of energy $\hbar\omega_0$ by the junction. The above equation shows that, in the high-gain limit, the SIS amplifier is near quantum-limited even in the presence of this quasiparticle noise. Thus, to mitigate the effects of the quasiparticle noise, the operational voltages of the device are such that these noise terms [three last terms of Eq. (10)] are much smaller than the parametric interaction. As illustrated in Fig. 1(b), the optimal dc-voltage lies in the interval $2(\Delta-\hbar\omega_0) < eV < 2\Delta-\hbar\omega_0$, where absorption and emission processes by the junction, $\propto \mathrm{Re}Y_0(\omega)$, are weak and parametric interaction, $\propto Y_1(\omega)$, is dominant.

For $\omega = 0$, $\hat{a}_{\rm in}[\omega_0]$ and $\hat{a}^\dagger_{\rm in}[\omega_0]$ do not commute, and the first two terms of Eq. (9) rather characterize an ideal phase-sensitive amplifier [44, 45]. In this operational mode, the gain G_0 is defined as a combination of r_0, γ_0 and the phases of the input and output fields [23]. The added noise is given by a linear combination of the two last terms of Eq. (9) and it also depends on the input and output field phases [23].

To better characterize the radiation emitted by the SIS amplifier, we also compute the output power spectrum $S_\theta(\omega)$, defined in terms of $\langle\Delta\hat{X}_\theta[\omega]\Delta\hat{X}_\theta[\omega']\rangle = S_\theta(\omega)\delta(\omega+\omega')$, with $\hat{X}_\theta[\omega] = e^{-i\theta}\hat{a}_{\rm out}[\omega+\omega_0] + e^{i\theta}\hat{a}^\dagger_{\rm out}[\omega_0-\omega]$ the output field quadrature with fluctuations $\Delta\hat{X}_\theta[\omega] = \hat{X}_\theta[\omega] - \langle\hat{X}_\theta[\omega]\rangle$ and θ the phase of the output field. Similarly to amplification, the emitted radiation can be also characterized by single-mode $S_\theta(\omega=0) < 1$ or two-mode $S_\theta(\omega\neq 0) < 1$ squeezed state.

It is worth mentioning that to derive Eq. (9) we neglected conversion processes where photons of frequency $|\omega| > 2\omega_0$ are up- or down-converted to ω. This approximation is justified by the fact that the R_TC time of the junction acts as a high-frequency cutoff. For the results presented in the next section, we take $\omega_{RC} = 1/R_TC = 2\pi\times 30$ GHz as a fixed parameter of the junction, which is obtained for a normal state resistance $R_T = 50\Omega$ and $C = 100$ fF. In addition, a low-pass filter can be used to filter all frequencies above $2\omega_0$. Since we are interested in signals of frequency $\omega_0 \ll \Delta/\hbar$ amplified by operating the junction close to the onset of quasi-particle transport $eV \approx 2\Delta$, we also ignored current and noise terms originating from the tunneling of Cooper pairs whose Josephson frequency $\sim 4\Delta/\hbar \gg 2\omega_0$ would be efficiently filtered as well.

III. RESULTS

We first present results for an ideal SIS junction, with transport response rising steeply for voltages $eV = 2\Delta + n\hbar\omega_0$ as illustrated in Fig. 1(b). We then investigate how gain and squeezing properties are affected by low-frequency noise, which are smoothing out the transport response of the junction and, consequently, diminishing the strength of the parametric interaction.

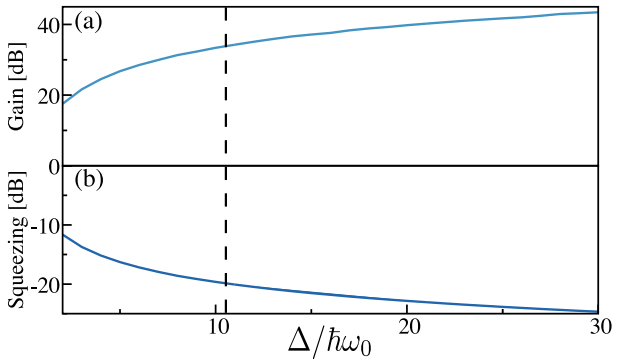

FIG. 2. (a) Phase-sensitive gain and (b) single-mode squeezing as a function of $\Delta/\hbar\omega_0$ for $\omega_0/2\pi = 4$ GHz. The dashed line marks the values for an Aluminum superconducting junction. For each value of $\Delta/\hbar\omega_0$ there are optimal ac- and dc-voltages that maximize single-mode squeezing. The optimal dc-voltage is always equal to $eV^{\rm opt} \lesssim 2\Delta - \hbar\omega_0$, while the optimal ac-voltage amplitude diminishes as $\Delta/\hbar\omega_0$ increases (not shown here).

A. Ideal SIS junction

Before turning to the full amplification and squeezing frequency dependences, we first present results for $\omega = 0$ which corresponds to the phase-sensitive mode. Figs. 2(a) and (b) illustrate, respectively, the phase-sensitive gain and single-mode squeezing as a function of $\Delta/\hbar\omega_0$, when optimizing V and $V_{\rm ac}$ to maximize single-mode squeezing. Here, Δ varies while $\omega_0/2\pi$ is kept fixed and equal to 4 GHz. Already at small $\Delta/\hbar\omega_0 \simeq 2$ we observe 15 dB of amplification and -10 dB of squeezing. As $\Delta/\hbar\omega_0$ increases, the strength of the nonlinearities giving rise to parametric interaction increases, thus enhancing gain and squeezing as illustrated in Fig. 2. This can be understood by the fact that $S_n(\omega)$ and, consequently, $Y_n(\omega)$ are proportional to Δ/R_T in the limit of $\Delta/\hbar\omega_0 \to \infty$. Thus, increasing Δ leads to an increase of the parametric interaction strength $\propto Y_1(\omega)$. For $\Delta/\hbar\omega_0 = 30$, amplification and squeezing reach 43 dB and -25 dB, respectively. In Fig. 2, the dashed-line corresponds to an Aluminum junction. As expected, the optimal dc-voltage is $eV^{\rm opt} \lesssim 2\Delta - \hbar\omega_0$ for all values of $\Delta/\hbar\omega_0$ (not shown). At this dc-voltage, the susceptance $\mathrm{Im}Y_1$ is larger than the dissipative contributions $\propto \mathrm{Re}Y_0$, thus making the parametric interaction the dominant process over dissipation, as illustrated in Fig. 1(b). It is interesting to note that $V^{\rm opt}$ is also the optimal operational point of SIS mixers [35]. On the other hand, the optimal ac-voltage $V^{\rm opt}_{\rm ac}$ decreases as $\Delta/\hbar\omega_0$ increases.

For the remainder of this article, we consider an Aluminum SIS junction with $\Delta/\hbar\omega_0 \approx 10.9$ for $\omega_0/2\pi = 4$ GHz. In the phase-sensitive mode ($\omega = 0$), gain and squeezing are respectively ~ 34 dB and ~ -20 dB at the optimal operational point ($eV^{\rm opt} \approx 20.762\times\hbar\omega_0$ and $eV^{\rm opt}_{\rm ac} \approx 0.06\times 2\hbar\omega_0$). Moreover, the noise added by tunneling of quasiparticles is of the order of 10^{-4} added photons, meaning that the amplifier operates near the quantum limit.

We now investigate the frequency dependence of phase-

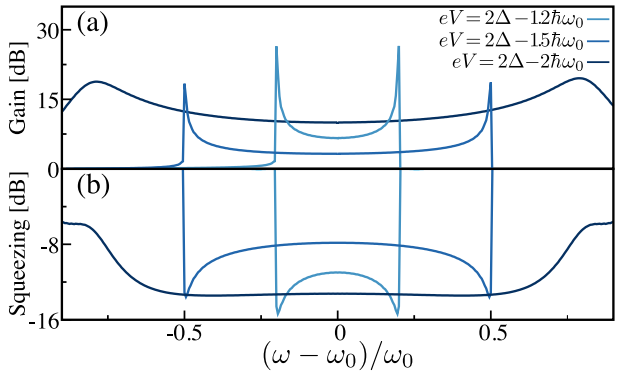

FIG. 3. Aluminum junction ($\Delta/\hbar\omega_0 \approx 10.9$): phase-preserving gain (a) and two-mode squeezing (b) as a function of the frequency detuning from the pump frequency $\omega_0/2\pi = 4$ GHz. We consider a fixed ac-voltage amplitude $V_{\rm ac} = 0.1 \times 2\hbar\omega_0$ for three different values of dc-voltages, $V \approx 2\Delta - 1.2\hbar\omega_0$ (cyan line), $V \approx 2\Delta - 1.5\hbar\omega_0$ (dark-blue line), and $V \approx 2\Delta - 2\hbar\omega_0$ (black line). At $\omega = \omega_0$, the amplifier is operated in the phase-sensitive mode.

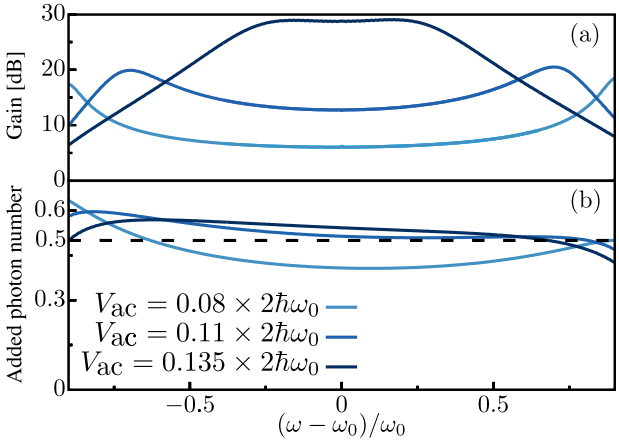

FIG. 4. Aluminum junction ($\Delta/\hbar\omega_0 \approx 10.9$): Gain spectrum (a) and added noise power spectral density (b) as a function of the frequency detuning from $\omega_0/2\pi = 4$ GHz for $V \approx 2\Delta - 2\hbar\omega_0$ and three different values of ac-voltage amplitude, $V_{\rm ac} \approx 0.08 \times 2\hbar\omega_0$ (cyan line), $V_{\rm ac} \approx 0.11 \times 2\hbar\omega_0$ (blue line), and $V_{\rm ac} \approx 0.135 \times 2\hbar\omega_0$ (black line). The dashed line marks the added noise for an ideal phase-preserving amplifier. In this case, half-photon is added during the amplification process. As the ac-voltage amplitude increases the gain increases and the bandwidth is reduced. However, the added noise still near the quantum limit for all values of $V_{\rm ac}$.

preserving gain and two-mode squeezing, and how they are controlled by dc- and ac-voltage amplitudes. First, we find that for the optimal voltages, $V^{\rm opt}$ and $V_{\rm ac}^{\rm opt}$, both gain and squeezing vanish at finite detuning ($\omega \neq 0$). This is explained by the fact that, at finite detuning, the absorption of single photons is the dominant process already for $eV = 2\Delta - \hbar(\omega+\omega_0) < V^{\rm opt}$, while parametric interaction is dominant for $eV \lesssim 2\Delta - \hbar(\omega+\omega_0)$. The response of the junction at finite detuning ω is similar to the one presented in Fig. 1(b). To achieve parametric amplification at finite detuning, we set dc-voltage to a value smaller than $V^{\rm opt}$. In this case, there is a frequency range $[e(V-V^{\rm opt})/\hbar, e(V^{\rm opt}-V)/\hbar]$ where the parametric interaction is the dominant mechanism, leading to phase-preserving amplification and two-mode squeezing at finite detuning. This frequency range defines the operational bandwidth of the device.

Figure 3(a) illustrates the phase-preserving gain while panel (b) shows two-mode squeezing as a function of the detuning $(\omega - \omega_0)/\omega_0$ for three different values of V and for fixed $eV_{\rm ac} = 0.1 \times 2\hbar\omega_0$. These results show striking features. The first is that the bandwidth is controlled by the dc-voltage and, as anticipated, equal to $2e(V^{\rm opt} - V)/\hbar$ for $2(\Delta-\hbar\omega_0) < eV < 2\Delta-\hbar\omega_0$. As expected, the largest bandwidth occurs for $eV \approx 2\Delta - 2\hbar\omega_0$. Both gain and squeezing spectra are flat over a 4 GHz band, with more than 10 dB of phase-preserving gain and -14 dB of squeezing. Moreover, the broadband squeezing spectrum characterizes the generation of far-separated two-mode squeezed states.

As mentioned before, the tunneling of quasiparticles also generates noise preventing the amplifier from operating at the quantum-limit. To further characterize the SIS junction parametric amplifier, we fix $eV \approx 2(\Delta - \hbar\omega_0)$ and investigate the impact of the ac-voltage amplitude on the gain and added noise. Figs. 4(a) and (b) illustrate the gain and added noise for three different values of $V_{\rm ac}$, respectively. The gain is observed to raise with increasing ac-voltage amplitude, while adding noise and decreasing the bandwidth. More importantly, gain can be significantly increased while the added noise remains of the same order. For instance, increasing $V_{\rm ac}$ from $0.11\times2\hbar\omega_0$ to $0.135\times2\hbar\omega_0$, the gain jumps from 14 dB to approximately 30 dB, while the added noise remains practically the same. The bandwidth is reduced with the increased gain, nonetheless it is of the same order of the measured bandwidth of the Josephson traveling wave parametric amplifier [27]. The increase of both gain and added noise is due to the enhancement of photon-assisted tunneling of quasiparticles, which controls both parametric amplification and added noise [three last terms of Eq. (10)]. However, even with the increase of the added noise with $V_{\rm ac}$, the SIS amplifier operates near the high-gain quantum limit of an ideal phase-preserving amplifier [dashed line in Fig. 4(b)] [44].

Finally, a higher degree of amplification and squeezing can be obtained by fabricating a junction with normal state resistance smaller than 50 Ω. However, due to the impedance mismatch between the junction and the TL, the bandwidth goes to zero as $R_{\rm T}$ diminishes. This can be understood by the fact that internal reflections of the microwave signal, caused by the large impedance mismatch, can interfere destructively, thereby destroying the coherent coupling between the signal ($\hat{a}_{\rm in}[\omega+\omega_0]$) and the idler ($\hat{a}_{\rm in}^\dagger[\omega_0-\omega]$) frequency modes. Also, as shown in Fig. 2, a SIS junction with large superconducting gap leads to higher gain and squeezing. For instance, a Niobium junction ($\Delta/h \sim 750$ GHz) would, in principle, generate higher gain and squeezing than an Aluminum junction.

Finally, a higher degree of amplification and squeezing can be obtained by fabricating a junction with normal state re-

sistance smaller than 50 Ω. However, due to the impedance mismatch between the junction and the TL, the bandwidth and gain goes to zero as $R_{\rm T}$ diminishes. Also, as shown in Fig. 2, a SIS junction with large superconducting gap leads to higher gain and squeezing. For instance, a Niobium junction ($\Delta/h \sim 750$ GHz) would, in principle, generate higher gain and squeezing than an Aluminum junction. Moreover, the operational bandwidth could be extended to the THz range with NbSi or NbN junctions.

B. Effects of low-frequency noise

The results presented in the previous section were obtained considering an ideal SIS junction in the low-temperature limit $k_{\rm B}T \ll 2\Delta$ for which the transport response rises steeply for $eV = 2\Delta + n\hbar\omega_0$ [33]. However, this is an idealized situation and, in practice, temperature or low-frequency noise can smoothen the transport response. Here, we consider the effects of low-frequency noise on gain and squeezing properties of the SIS amplifier. These effects are included by assuming that the junction interact with a low-frequency electromagnetic environment [46] and that the transport properties are described by the $P(E)$-theory [43]. Indeed, this approach has been shown to quantitatively explain the finite Dynes tunneling density of states, usually observed below the dc-transport gap in a normal-insulator-superconductor junctions and the corresponding smoothing of the BCS coherence peak [33, 47]. In this approach, the low-frequency noise modifies the equilibrium noise current noise to

$$S_{\rm eq}^{\rm eff}(\omega) = \int_{-\infty}^{\infty} S_{\rm eq}(\hbar\omega - E)P(E)dE, \qquad (11)$$

where $P(E)$ is the probability density of a tunneling electron emitting energy and takes the form for low-frequency noise [43]

$$P(E) = \frac{1}{\sqrt{4\pi E_c k_{\rm B}T}} \exp\left(-\frac{(E-E_c)^2}{4E_c k_{\rm B}T}\right), \qquad (12)$$

with $E_c = e^2/2C_{bt}$ is the capacitor charging energy. This model is justified by the fact that the low noise biasing scheme consists of a resistive voltage divider followed by large capacitive filtering [46, 48]. The low-frequency impedance is thus the parallel combination of a resistance with a large capacitance $C_{\rm bt}$. This filtering scheme reduces the bandwidth over which low-frequency voltage noise can develop to the kHz range [48], making the low-frequency voltage fluctuations fully classical. With this model, the theory developed in Sec. II remains the same except for the replacement of $S_{\rm eq}(\omega)$ by $S_{\rm eq}^{\rm eff}(\omega)$ in Eq. (8).

Figure 5 illustrates the resulting effect on both (a) gain and (b) squeezing for $C_{\rm bt} \sim 1$ nF (dark-blue line) and $C_{\rm bt} \sim 10$ pF (light-blue line) corresponding to an efficient and inefficient low-frequency noise filtering scheme, respectively. These results are compared with the ideal case (dashed-line), where the junction does not interact with the low-frequency environment. For an Aluminum junction ($\Delta/\hbar\omega_0 \approx 10.9$) and

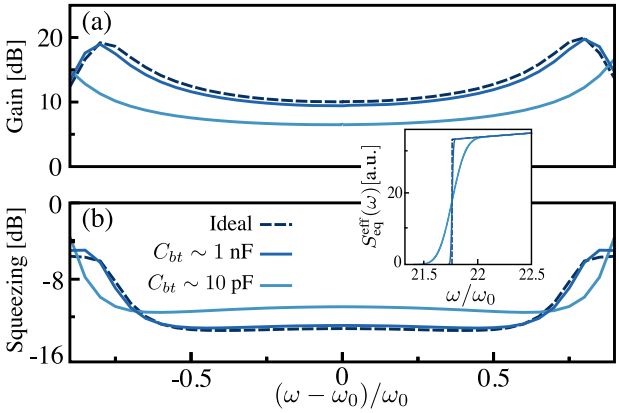

FIG. 5. Aluminum junction ($\Delta/\hbar\omega_0 \approx 10.9$): Gain (a) and squeezing (b) as a function of frequency detuning in the presence (solid lines) and in the absence (dashed line) of low-frequency electromagnetic environment. The two solid lines illustrate an efficient ($C_{\rm bt} \sim 1$ nF - blue line) and inefficient ($C_{\rm bt} \sim 10$ pF - cyan line) low-frequency noise filtering scheme. As expected, for an efficient filtering scheme, both gain and squeezing are quantitatively equal to the result obtained in absence of low-frequency electromagnetic environment.

$T = 15$ mK, $C_{\rm bt} \sim 1$ nF corresponds to rms voltage fluctuations of $\sqrt{k_{\rm B}T/2C_{\rm bt}} \sim 11$ nV (dark-blue line), the gain and squeezing are only weakly affected by the low-frequency environment which is efficiently filtered. The effect of low-frequency noise on $S_{\rm eq}^{\rm eff}(\omega)$ is illustrated in the inset of Fig. 5. For $C_{\rm bt} \sim 1$ nF, $S_{\rm eq}^{\rm eff}(\omega)$ is almost indistinguishable from the ideal case (dashed line), a signature that the low-frequency noise is efficiently filtered. On the other hand, under less efficient filtering, $C_{bt} \sim 10$ pF corresponding to ~ 0.1 μV rms voltage fluctuations (light-blue line), the equilibrium current noise rises smoothly and its behavior near $2\Delta/\hbar$ deviates from the ideal case (see inset). In this case, low-frequency noise diminishes both gain and squeezing amplitudes (light-blue line). However, the bandwidth is only weakly modified.

IV. CONCLUSIONS

We have proposed a near-quantum-limited broadband amplifier and squeezer based on the photon-assisted tunneling of quasiparticles in a SIS junction. This device can function as a phase-sensitive or phase-preserving amplifier. The gain can be tuned by the dc- and ac-voltages amplitude to reach 30 dB over 2 GHz or 14 dB over 4 GHz. This device is also a source of two-mode squeezing with bandwidth over more than 4 GHz and -14 dB of squeezing. Moreover, gain and two-mode squeezing can be fine -tuned in-situ by changing the pumping tone frequency and dc-voltage bias. Therefore, the design and fabrication simplicity of this SIS amplifier, together with its operational mode flexibility, makes it a versatile near-quantum-limited microwave amplifier and squeezer, which can be easily integrated in many quantum microwaves experiments.

ACKNOWLEDGMENTS

UCM thank S. Boutin, A. L. Grimsmo and M. Westig for fruitful discussion, and the Quantronics group for hospitality. UCM and AB were supported from Canada First Research Excellence Fund and NSERC. BR was supported by Canada Excellence Research Chairs, Government of Canada, Natural Sciences and Engineering Research Council of Canada, Québec MEIE, Québec FRQNT via INTRIQ, Université de Sherbrooke via EPIQ, and Canada Foundation for Innovation. The research at CEA-Saclay has received funding from the European Research Council under the European Unions Programme for Research and Innovation (Horizon 2020)/ERC Grant Agreement No. 639039, and support from the ANR AnPhoTeQ research contract.

[1] A. Wallraff, D. I. Schuster, A. Blais, L. Frunzio, R.-S. Huang, J. Majer, S. Kumar, S. M. Girvin, and R. J. Schoelkopf, "Strong coupling of a single photon to a superconducting qubit using circuit quantum electrodynamics," Nature **431**, 162 (2004).

[2] M. A. Castellanos-Beltran and K. W. Lehnert, "Widely tunable parametric amplifier based on a superconducting quantum interference device array resonator," Appl. Phys. Lett. **91**, 083509 (2007).

[3] N. Bergeal, F. Schackert, M. Metcalfe, R. Vijay, V. E. Manucharyan, L. Frunzio, D. E. Prober, R. J. Schoelkopf, S. M. Girvin, and M. H. Devoret, "Phase-preserving amplification near the quantum limit with a josephson ring modulator," Nature **465**, 64 (2010).

[4] X. Zhou, V. Schmitt, P. Bertet, D. Vion, W. Wustmann, V. Shumeiko, and D. Esteve, "High-gain weakly nonlinear flux-modulated josephson parametric amplifier using a squid array," Phys. Rev. B **89**, 214517 (2014).

[5] C. Eichler, Y. Salathe, J. Mlynek, S. Schmidt, and A. Wallraff, "Quantum-limited amplification and entanglement in coupled nonlinear resonators," Phys. Rev. Lett. **113**, 110502 (2014).

[6] F. Mallet, F. R. Ong, A. Palacios-Laloy, F. Nguyen, P. Bertet, D. Vion, and D. Esteve, "Single-shot qubit readout in circuit quantum electrodynamics," Nat. Physics **5**, 791 (2009).

[7] T. Walter, P. Kurpiers, S. Gasparinetti, P. Magnard, A. Potocnik, Y. Salathé, M. Pechal, M. Mondal, M. Oppliger, C. Eichler, and A. Wallraff, "Rapid high-fidelity single-shot dispersive readout of superconducting qubits," Phys. Rev. Applied **7**, 054020 (2017).

[8] Eva Zakka-Bajjani, J. Dufouleur, N. Coulombel, P. Roche, D. C. Glattli, and F. Portier, "Experimental determination of the statistics of photons emitted by a tunnel junction," Phys. Rev. Lett. **104**, 206802 (2010).

[9] G. Gasse, C. Lupien, and B. Reulet, "Observation of squeezing in the electron quantum shot noise of a tunnel junction," Phys. Rev. Lett. **111**, 136601 (2013).

[10] J. Stehlik, Y.-Y. Liu, C. M. Quintana, C. Eichler, T. R. Hartke, and J. R. Petta, "Fast charge sensing of a cavity-coupled double quantum dot using a josephson parametric amplifier," Phys. Rev. Applied **4**, 014018 (2015).

[11] M. Westig, B. Kubala, O. Parlavecchio, Y. Mukharsky, C. Altimiras, P. Joyez, D. Vion, P. Roche, D. Esteve, M. Hofheinz, M. Trif, P. Simon, J. Ankerhold, and F. Portier, "Emission of nonclassical radiation by inelastic cooper pair tunneling," Phys. Rev. Lett. **119**, 137001 (2017).

[12] J. O. Simoneau, S. Virally, C. Lupien, and B. Reulet, "Photon-pair shot noise in electron shot noise," Phys. Rev. B **95**, 060301 (2017).

[13] A. Bienfait, P. Campagne-Ibarcq, A. H. Kiilerich, X. Zhou, S. Probst, J. J. Pla, T. Schenkel, D. Vion, D. Esteve, J. J. L. Morton, K. Moelmer, and P. Bertet, "Magnetic resonance with squeezed microwaves," Phys. Rev. X **7**, 041011 (2017).

[14] B. M. Brubaker, L. Zhong, Y. V. Gurevich, S. B. Cahn, S. K. Lamoreaux, M. Simanovskaia, J. R. Root, S. M. Lewis, S. Al Kenany, K. M. Backes, I. Urdinaran, N. M. Rapidis, T. M. Shokair, K. A. van Bibber, D. A. Palken, M. Malnou, W. F. Kindel, M. A. Anil, K. W. Lehnert, and G. Carosi, "First results from a microwave cavity axion search at 24 μeV," Phys. Rev. Lett. **118**, 061302 (2017).

[15] M. A. Castellanos-Beltran, K. D. Irwin, G. C. Hilton, L. R. Vale, and K. W. Lehnert, "Amplification and squeezing of quantum noise with a tunable josephson metamaterial," Nat. Physics **4**, 929 (2008).

[16] K. W. Murch, S. J. Weber, K. M. Beck, E. Ginossar, and I. Siddiqi, "Reduction of the radiative decay of atomic coherence in squeezed vacuum," Nature **499**, 62 (2013).

[17] D. M. Toyli, A. W. Eddins, S. Boutin, S. Puri, D. Hover, V. Bolkhovsky, W. D. Oliver, A. Blais, and I. Siddiqi, "Resonance fluorescence from an artificial atom in squeezed vacuum," Phys. Rev. X **6**, 031004 (2016).

[18] N. Didier, A. Kamal, W. D. Oliver, A. Blais, and A. A. Clerk, "Heisenberg-limited qubit read-out with two-mode squeezed light," Phys. Rev. Lett. **115**, 093604 (2015).

[19] S. Puri and A. Blais, "High-fidelity resonator-induced phase gate with single-mode squeezing," Phys. Rev. Lett. **116**, 180501 (2016).

[20] B. Royer, A. L. Grimsmo, N. Didier, and A. Blais, "Fast and high-fidelity entangling gate through parametrically modulated longitudinal coupling," Quantum **1**, 11 (2017).

[21] S. L. Braunstein and P. van Loock, "Quantum information with continuous variables," Rev. Mod. Phys. **77**, 513–577 (2005).

[22] A. L. Grimsmo and A. Blais, "Squeezing and quantum state engineering with josephson travelling wave amplifiers," npj Quantum Information **3**, 20 (2017).

[23] S. Boutin, D. M. Toyli, A. V. Venkatramani, A. Eddins, I. Siddiqi, and A. Blais, "Effect of higher-order nonlinearities on amplification and squeezing in josephson parametric amplifiers," Physics Review Applied **8**, 054030 (2017).

[24] J. Y. Mutus, T. C. White, R. Barends, Y. Chen, Z. Chen, B. Chiaro, A. Dunsworth, E. Jeffrey, J. Kelly, A. Megrant, C. Neill, P. J. J. O'Malley, P. Roushan, D. Sank, A. Vainsencher, J. Wenner, K. M. Sundqvist, A. N. Cleland, and J. M. Martinis, "Strong environmental coupling in a josephson parametric amplifier," Appl. Phys. Lett. **104**, 263513 (2014).

[25] T. Roy, S. Kundu, M. Chand, A. M. Vadiraj, A. Ranadive, N. Nehra, M. P. Patankar, J. Aumentado, A. A. Clerk, and R. Vijay, "Broadband parametric amplification with impedance engineering: Beyond the gain-bandwidth product," Appl. Phys. Lett. **107**, 262601 (2015).

[26] M. P. Westig and T. M. Klapwijk, "Josephson parametric reflection amplifier with integrated directionality," arXiv:1706.09300v1 (2017).

[27] C. Macklin, K. O'Brien, D. Hover, M. E. Schwartz, V. Bolkhovsky, X. Zhang, W. D. Oliver, and I. Siddiqi, "A near–quantum-limited josephson traveling-wave parametric amplifier," Science **350**, 307 (2015).

[28] C. W. J. Beenakker and H. Schomerus, "Antibunched photons emitted by a quantum point contact out of equilibrium," Phys. Rev. Lett. **93**, 096801 (2004).

[29] A. D. Armour, M. P. Blencowe, E. Brahimi, and A. J. Rimberg, "Universal quantum fluctuations of a cavity mode driven by a josephson junction," Phys. Rev. Lett. **111**, 247001 (2013).

[30] Juha Leppäkangas, Mikael Fogelström, Alexander Grimm, Max Hofheinz, Michael Marthaler, and Göran Johansson, "Antibunched photons from inelastic cooper-pair tunneling," Phys. Rev. Lett. **115**, 027004 (2015).

[31] U. C. Mendes and C. Mora, "Cavity squeezing by a quantum conductor," New J. Phys. **17**, 113014 (2015).

[32] U. C. Mendes and C. Mora, "Electron-photon interaction in a quantum point contact coupled to a microwave resonator," Phys. Rev. B **93**, 235450 (2016).

[33] A. Barone and G. Paterno, *Physcs and applications of the Josephson effect* (A Wiley-Interscience publication, 1982).

[34] G. S. Lee, "Superconductor-insulator-superconductor reflection parametric amplifier," Appl. Phys. Lett. **41** (1982), 10.1063/1.93468.

[35] J. R. Tucker and M. J. Feldman, "Quantum detection at millimeter wavelengths," Rev. Mod. Phys. **57**, 1055 (1985).

[36] I. A. Devyatov, L. S. Kuzmin, K. K. Likharev, V. V. Migulin, and A. B. Zorin, "Quantum-statistical theory of microwave detection using superconducting tunnel junctions," Journal of Applied Physics **60**, 1808 (1986).

[37] Bernard Yurke and John S. Denker, "Quantum network theory," Phys. Rev. A **29**, 1419–1437 (1984).

[38] P. K. Tien and J. P. Gordon, "Multiphoton process observed in the interaction of microwave fields with the tunneling between superconductor films," Phys. Rev. **129**, 647–651 (1963).

[39] C. W. Gardiner and M. J. Collett, "Input and output in damped quantum systems: Quantum stochastic differential equations and the master equation," Phys. Rev. A **31**, 3761–3774 (1985).

[40] M. H. Devoret, D. Esteve, H. Grabert, G.-L. Ingold, H. Pothier, and C. Urbina, "Effect of the electromagnetic environment on the coulomb blockade in ultrasmall tunnel junctions," Phys. Rev. Lett. **64**, 1824–1827 (1990).

[41] A. L. Grimsmo, F. Qassemi, B. Reulet, and A. Blais, "Quantum optics theory of electronic noise in coherent conductors," Phys. Rev. Lett. **116**, 043602 (2016).

[42] C. Mora, C. Altimiras, P. Joyez, and F. Portier, "Quantum properties of the radiation emitted by a conductor in the coulomb blockade regime," Phys. Rev. B **95**, 125311 (2017).

[43] G.-L. Ingold and Yu. V. Nazarov, *Single Charge Tunneling*, edited by H. Grabert and M.H. Devoret (Plenum Press, New York, 1992).

[44] A. A. Clerk, M. H. Devoret, S. M. Girvin, F. Marquardt, and R. J. Schoelkopf, "Introduction to quantum noise, measurement, and amplification," Rev. Mod. Phys. **82**, 1155 (2010).

[45] C. M. Caves, "Quantum limit on noise in linear amplifiers," Phys. Rev. D **26**, 1817 (1982).

[46] M. Hofheinz, F. Portier, Q. Baudouin, P. Joyez, D. Vion, P. Bertet, P. Roche, and D. Esteve, "Bright side of the coulomb blockade," Phys. Rev. Lett. **106**, 217005 (2011).

[47] J. P. Pekola, V. F. Maisi, S. Kafanov, N. Chekurov, A. Kemppinen, Yu. A. Pashkin, O.-P. Saira, . Möttönen, and J. S. Tsai, "Environment-assisted tunneling as an origin of the dynes density of states," Phys. Rev. Lett. **105**, 026803 (2010).

[48] F. Chen, J. Li, A. D. Armour, E. Brahimi, J. Stettenheim amd A. J. Sirois amd R. W. Simmonds, M. P. Blencowe, and A. J. Rimberg, "Realization of a single-cooper-pair josephson laser," Phys. Rev. B **90**, 020506 (2014).